*Macromolecules* **1981**, *14*, 1779–1784

# Pulsed NMR Studies of Crystalline-State Extrusion of High-Density Polyethylene

**Masayoshi Ito, Tetsuo Kanamoto, and Koji Tanaka**

*Department of Chemistry, Faculty of Science, Science University of Tokyo, Kagurazaka, Shinjuku-ku, Tokyo 162, Japan*

**Roger S. Porter***

*Materials Research Laboratory, Polymer Science and Engineering Department, University of Massachusetts, Amherst, Massachusetts 01003.*

*Received December 15, 1980*

ABSTRACT: Proton spin–spin relaxation times ($T_2$) have been measured as a function of temperature for high-density polyethylene extrudates prepared at 90 and 110 °C having nominal extrusion draw ratios (EDR) up to 35. Below about 90 °C, the decay signals showed a complex beat structure and the measurements were therefore limited to temperatures above 90 °C. Three relaxation times, $T_{2a}$ (the longest), $T_{2i}$ (intermediate), and $T_{2c}$ (the shortest), were observed for extrudates having EDR ≤ 12 and are ascribed to the relaxation from amorphous, intermediate, and rigid (crystalline) components in the samples. For highly drawn samples with EDR ≥ 25 only two $T_2$'s ($T_{2a}$ and $T_{2c}$) were observed below melting. The structural change during extrusion in the noncrystalline regions was sensitively detected by $T_{2a}$. $T_{2a}$ decreases very rapidly with increasing EDR and approaches a limiting value at EDR > 20. The extrusion at a lower temperature produced more constraint on the noncrystalline component. The results have the important implication that the structure of noncrystalline regions rapidly changes with increasing EDR and approaches a limiting structure at EDR > 20, which changes slightly depending on the extrusion conditions. Additional increase in EDR does not significantly alter the structure of noncrystalline regions in those samples extruded below 110 °C. The fraction of $T_{2c}$ component was in good agreement with the mass fraction crystallinity estimated from the heat of fusion of the samples irrespective of the EDR and increased with EDR. The thermal stability of the extrudates increases with EDR and no appreciable annealing was observed below 130 °C for the sample with the highest EDR (EDR = 35).

## Introduction

The ultradrawing of linear high-density polyethylene (HDPE) achieved by different techniques produces a unique morphology which exhibits unusually high crystalline orientation,[1] tensile modulus and strength,[2–6] birefringence,[1,3] in some cases transparency,[7,8] large superheating,[9,10] and negative thermal expansion.[3,11] Among these properties, the enhancement of mechanical properties has been one of central interest. The modulus of the fibers and films of HDPE drawn by crystalline-state extrusion[2,12] as well as conventional drawing[5,13] exhibits a characteristic change with deformation ratio (DR); i.e., it increases with DR slowly at low DR and then more rapidly and steadily at higher DR. The DR dependence of the structure and properties have been extensively studied by Porter et al.[2,3] and Takayanagi et al.[14,15] for solid-state extrusion. The observed macroscopic structure, properties such as crystallinity, and chain orientation in both crystalline and amorphous regions do not give the full answer to the characteristic change of modulus with DR. The important role of noncrystalline regions which connect two or more crystallites along the fiber direction has been emphasized.[16,17] However, less information has been obtained for the structural and property changes in noncrystalline regions as compared with crystalline regions.

Pulsed NMR studies of semicrystalline polymers have often been used as one of the most effective techniques for obtaining direct information about the molecular motions and structural changes of each phase.[18–20] In the present work, proton spin–spin relaxation times ($T_2$) of crystalline-state extruded HDPE having an extrusion draw ratio (EDR) up to 35 have been measured by the solid echo NMR technique[21] as a function of temperature. Two and three $T_2$ values corresponding to molecular segments having different mobility have been observed depending on EDR and temperature. The relaxation time from amorphous regions ($T_{2a}$) drastically changed with EDR, suggesting a high sensitivity of $T_{2a}$ to the structural change in amorphous regions. Thus, the structural change during crystalline-state extrusion of HDPE will be discussed on the basis of $T_2$ values (segmental mobility) and the fractions of $T_{2a}$ (amorphous), $T_{2i}$ (intermediate), and $T_{2c}$ (rigid or crystalline) components, as well as their dependence of the extrusion temperature and measurement temperature.

## Experimental Section

**Samples.** A linear high-density polyethylene, HDPE (du Pont Alathon 7050, $M_w$ = 58 000, $M_w/M_n$ = 3.0), was extruded on an Instron capillary rheometer by crystalline-state coextrusion[22] at extrusion temperatures of $T_E$ = 90 and 110 °C. A melt-crystallized billet of the HDPE, prepared by compression molding in vacuo, was split longitudinally into two halves having a smooth surface. One or more polymer films were sandwiched between the split billet halves, and the assembly was coextruded through brass conical dies which had an included entrance angle of 20° and nominal extrusion draw ratios (EDR) of 6, 12, 25, and 35. The nominal EDR was defined as the ratio of entrance to exit cross-sectional area of a die. The extrudates from the split billet halves only were used in this work. The extruded films obtained simultaneously were used for another study.

The melt-crystallized isotropic sample (MG) was prepared as follows: after NMR measurements of an extruded sample, the sample was melted at 140 °C for 30 min and then slowly cooled to room temperature. Therefore, the MG sample had a thermal history somewhat different from that of the initial solid billit used for solid-state extrusion.

**Measurements.** Pulsed NMR experiments were carried out with a JEOL pulsed NMR (JSE-5B) spectrometer operating at a frequency of 60 MHz. The solid echo sequence[21] 90°–$\tau$–90° (90° phase shift) provided an approximation of the complete free induction decay, from which spin–spin relaxation time ($T_2$) was obtained. In this study, $\tau$ and the pulse width have been adjusted to be 7 and 2 μs, respectively. Solid echo signals were collected and integrated with an Iwatsu DM-701 digitizer and an integrator which was constructed in our laboratory. When spectra with sufficient signal to noise were obtained by the addition of 30–40 scans, they were read out on a pen recorder. The extrudate fiber was cut into small pieces, about 2 mm long, that were randomly packed in a sample tube in vacuo. No anisotropy was observed in the free induction decay signal for these randomly packed

0024-9297/81/2214-1779$01.25/0

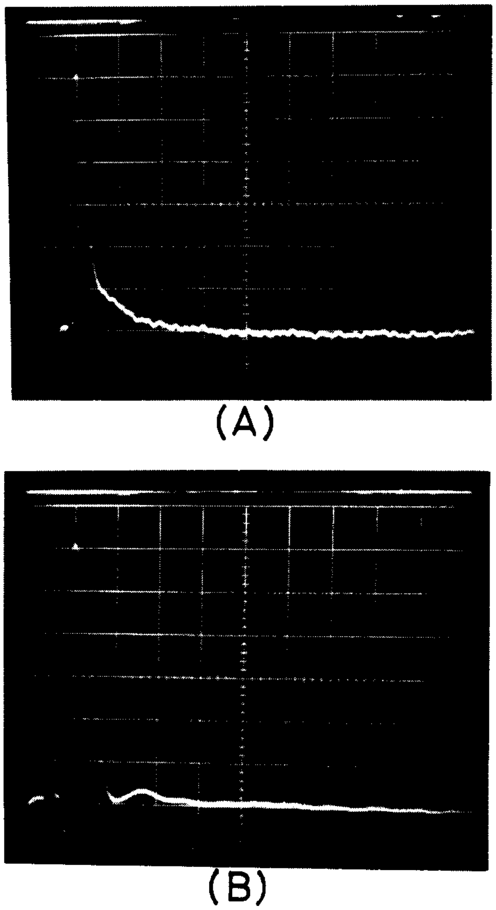

**Figure 1.** Photographs of solid echo signals (1 scan) from the extrudate with an EDR of 6: (A) 106 °C, $x$ = 50 μs/unit; (B) 24 °C, $x$ = 20 μs/unit. Note that integrated decay signals, as shown in Figure 2, were used for the decomposition of the curve.

samples. The temperature was controlled to an accuracy of ±0.5 °C by a gas-flow thermostat with a copper–constantan thermocouple. Estimated errors in the values of relaxation time and fraction were in the range 3–6%, as judged by the reproducibility of the data.

The melting temperature and heat of fusion of the samples were measured in a nitrogen atmosphere with a Perkin-Elmer differential scanning calorimeter (DSC-1B). The heating rate was 8 °C/min and the sample size was ~1 mg. The temperature and heat of fusion were calibrated against indium ($T_m$ = 156.4 °C, $\Delta H_f$ = 6.79 cal/g). The melting peak temperature and heat of fusion were reproducible for the same sample to within ±0.5 °C and ±3%, respectively. The crystalline mass fraction of the sample was calculated from the observed heat of fusion by assuming 69 cal/g[23] for the heat of fusion of a perfect crystal of polyethylene.

## Results and Discussion

Typical examples of the solid echo decay signals obtained for the extrudate with EDR 6 at 106 and 24 °C are shown in Figure 1. It is immediately apparent from Figure 1A, and much earlier work, that the observed decay is neither a single-exponential function nor a Gaussian function but their composite, indicative of the coexsistence of multiple phases (or domains) having different mobilities in the sample. A beat signal (Figure 1B) was observed at temperatures below about 90 °C in every sample. This type of signal has been observed in many semicrystalline polymers[18,20] in the temperature region where the molecular motions of the noncrystalline regions are not sufficiently activated. No convenient analytical method for this beat signal has been reported. Therefore, the experiments were carried out in temperature regions where decay signals are decomposable into Gaussian and/or exponential functions.

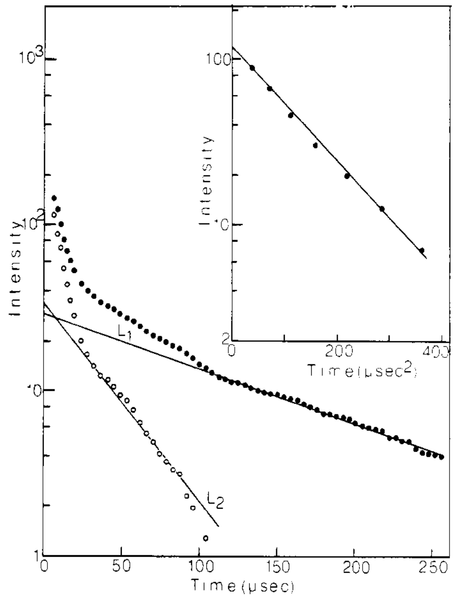

**Figure 2.** Analysis of the solid echo decay of the extrudate with an EDR of 6 at 112 °C.

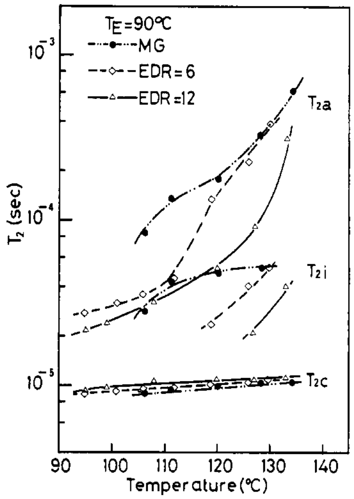

**Figure 3.** Temperature dependence of $T_2$ for the EDR 6 and EDR 12 extrudates and a melt-grown isotropic sample (MG). The extrusion temperature was 90 °C.

**Component Resolution of Signal Decay.** The signal intensities of the extrudate with an EDR of 6 at 112 °C are plotted against time in Figure 2. This decay curve was obtained by the addition of 30 scans of sufficient signal-to-noise ratio. For times greater than about 120 μs, the experimental points fall on a single straight line ($L_1$). To examine the portion of the curve which deviates from the line $L_1$, $L_1$ was extrapolated to zero time and the appropriate value substracted from the data. For times greater than about 30 μs, the subtraction is designated by open circles in Figure 2; these also fall on a straight line ($L_2$). Further, to examine the initial portion of the curve which deviates from $L_2$, $L_2$ was extrapolated to zero time and the appropriate value again subtracted from the curve. The initial portion of the data treated in this manner is shown in the upper region of Figure 2 plotted against time squared. All the solid echo decays obtained in this study were analyzed in this manner.

**Temperature Dependence of Spin–Spin Relaxation Time.** Figures 3 and 4 show spin–spin relaxation times as a function of temperature for extrudates with various

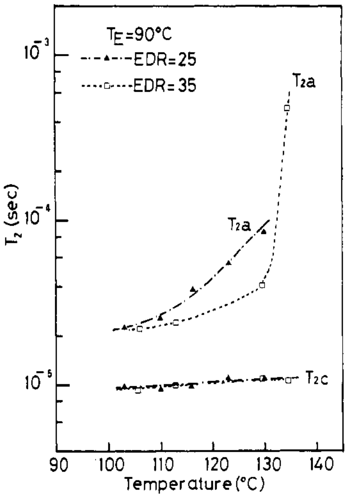

**Figure 4.** Temperature dependence of $T_2$ for the extrudates with EDR 25 and 35. The extrusion temperature was 90 °C.

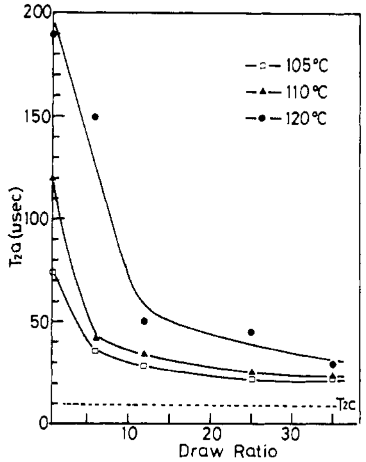

**Figure 5.** EDR dependence of $T_{2a}$ for the extrudates at 105, 110, and 120 °C. The value of $T_{2c}$ is shown by the dotted line. These samples were extruded at 90 °C.

EDR prepared at 90 °C and a melt-crystallized isotropic sample (MG). The EDR 6 and EDR 12 extrudates and MG exhibit three different $T_2$'s. The longest, intermediate, and the shortest relaxation times are denoted $T_{2a}$, $T_{2i}$, and $T_{2c}$, respectively. In the EDR 25 and EDR 35 samples, the $T_{2i}$ component could not be separated from the decay signal. The shortest relaxation time, $T_{2c}$, is associated with the crystalline region of the sample, as suggested by a Gaussian function of the decay, and the fraction of this component corresponds to the crystalline mass fraction calculated from the heat of fusion of the sample, as will be discussed later. $T_{2c}$ increased slightly with temperature in all the extrudates and the MG sample, and no significant difference was observed in the $T_{2c}$ vs. temperature curves. However, note that the extrudates having an EDR less than 12 showed a slightly longer $T_{2c}$ than the highly drawn extrudates and the isotropic sample. The small increase in $T_{2c}$ with temperature may be related mainly to the thermal expansion of the crystal lattice, which is influenced by crystalline imperfection.

The longest relaxation time, $T_{2a}$, which follows an exponential function, is ascribed to the relaxation of molecules that are motionally activated, on the NMR time scale, in the noncrystalline regions of the samples. $T_{2a}$ changes remarkably with the EDR of the samples. Figure 5 shows that $T_{2a}$ of the extrudates as a function of EDR, observed at 105, 110, and 120 °C. Although the thermal stability of the extrudates was lower for extrudates having lower EDR, as will be described later, the structural reorganization during NMR measurements was not significant at temperatures below 105 °C. At EDR $< 12$, $T_{2a}$ decreases very rapidly with increasing EDR and increases remarkably with measurment temperature. At higher EDR, $T_{2a}$ reaches a limiting value and the effect of EDR and temperature on $T_{2a}$ becomes less prominent (Figure 5). The results indicate that the constraint on the segmental mobility of the noncrystalline component increases rapidly with EDR at EDR $< 12$ and approaches a limiting value at EDR $> 12$.

Birefringence,[1,3,24] infrared dichroism,[25] thermal expansion,[3,11] amorphous density from small-angle X-ray scattering,[26] and diffusion rate of low molecular weight materials[27] have been used in efforts to study the structure and properties of the noncrystalline component of ultraoriented high-modulus polyethylene in terms of the amorphous orientation. Each technique has given some information about the noncrystalline component. Nevertheless, the structure and properties of the amorphous component in drawn semicrystalline polymers have not been well understood. The NMR method used in this work provides direct information about the segmental mobility of the noncrystalline component as well as its fraction. It is noteworthy that the change of $T_{2a}$ with EDR is very similar to that in amorphous orientation vs. EDR estimated from birefringence and thermal expansion coefficient of the amorphous component. This suggests that the constraint on the segmental mobility in the noncrystalline component increases in parallel with the degree of chain orientation in this component. Furthermore, the amorphous structure changes drastically by deformation at low EDR ($<10$) and reaches a limiting structure at higher EDR. This has an important implication in understanding the characteristic changes of tensile modulus with EDR in terms of the corresponding change in morphology. Many publications report that the orientation of the molecular axis in the crystalline phase increases with EDR in a way similar to that for the structural change in the amorphous regions. However, the tensile modulus along the fiber axis increases slowly in spite of the rapid structural changes in both the amorphous and crystalline regions at low EDR.[3,11] Thereafter the modulus increases more rapidly and steadily with EDR, where no significant orientation change is detected in either phase. Therefore the modulus increase cannot be directly correlated with chain orientation along the draw direction. Peterlin[16,17] proposed a molecular model which explains well the modulus increase with increasing DR. The model is based on the morphological change during deformation. His model contains two assumptions; one is that there is an increase in the taut tie molecule content (or crystalline bridges) connecting, longitudinally, crystallites at the lateral surface of the fibrils with DR, and the second is that the structure of the noncrystalline regions, existing between two crystalline blocks in a microfibril, does not change significantly at higher DR. The present NMR results support the latter assumption that the molecular constraint on the noncrystalline component approaches a limit at a higher EDR. The intermediate relaxation time, $T_{2i}$, was observed for an isotropic sample and extrudates having lower EDR ($\leq 12$) only at high temperature (Figure 3). Although $T_{2i}$ follows an exponential function (Figure 2), the value is short compared with $T_{2a}$ of the same sample at a given temperature. This indicates that the segmental motions responsible for $T_{2i}$ are fairly restricted. The lowest temperature where the $T_{2i}$ component appeared first is around 105 °C for the isotropic sample. With increasing

Table I
Characterization of Samples Extruded at 90 °C

| sample | $T_m$,[a] °C | $\Delta H_f$,[b] cal/g | $X_c$,[c] % | $T_{2c}$ fraction, % | $f_c$[d] |
|---|---|---|---|---|---|
| MG | | 49.0 | 71 | 71 | 0 |
| EDR 6 | 131.4 | 46.2 | 67 | 66 | 0.883 |
| EDR 12 | 134.0 | 47.6 | 69 | 72 | 0.987 |
| EDR 25 | 136.3 | 53.8 | 78 | 78 | 0.993 |
| EDR 35 | 135.9 | 55.9 | 81 | 86 | 0.994 |

[a] Melting peak temperature obtained by DSC at heating rate of 8 °C/min. [b] Heat of fusion of the samples obtained by DSC. [c] Crystalline mass fraction calculated from $\Delta H_f$. [d] Crystalline *c*-axis orientation function obtained by wide-angle X-ray azimuthal scan.

EDR this temperature shifted upward and at EDR ≥ 25 the $T_{2i}$ component was no longer observed below the melting temperature (Figures 3 and 4). Furthermore, around this temperature, $T_{2a}$ begins to increase rapidly with temperature, while $T_{2c}$ remains around 10 μs. Thus, the intermediate component becomes distinguished from the highly mobile component ($T_{2a}$ component) when the molecular motions of the relaxed segments are sufficiently activated while those of the constrained segments in the noncrystalline regions are not so active. Furthermore, the temperature dependence of $T_{2i}$ for the extrudates having lower EDR is remarkably different from that for the isotropic sample. This suggests an increased initial constraint on the structure of partially constrained segments. This interpretation is consistent with the fact that the samples having higher EDR showed no $T_{2i}$ because the noncrystalline segments in these samples are subject to considerable constraint, as suggested by the shorter $T_{2a}$.

**Fraction of $T_{2c}$ Component.** In order to discuss the structural changes during solid-state extrusion, the mass fraction of each component was determined from the values at the intersection of the vertical axis (time $t = 0$) and each straight line obtained by the decomposition procedure. The temperature dependence of the $T_{2c}$ fraction for the extrudates prepared at 90 °C and the MG sample is shown in Figure 6. The low-temperature plateau values of the $T_{2c}$ component are shown in Table I. Except for the MG sample, the magnitude increases with EDR, in agreement with previous results that the crystallinity increases with EDR.[3,28] It should be remembered that the MG sample was crystallized under conditions somewhat different from those for the initial billets from which these extrudates were prepared. The melting peak temperature and crystalline mass fractions calculated from heat of fusion are shown in Table I. Factors such as amorphous orientation, excess enthalpy of crystal surface, and crystalline imperfections may have, in some cases, a significant influence on the observed heat of fusion of drawn and extruded polyethylene.[29,30] It is noted, however, that the mass fraction crystallinity obtained from the heat of fusion is in good agreement with the fraction of the $T_{2c}$ component before annealing takes place. This is also true for the isotropic sample as well as the extrudate with the highest EDR, where the maximum orientation in the noncrystalline regions is expected.

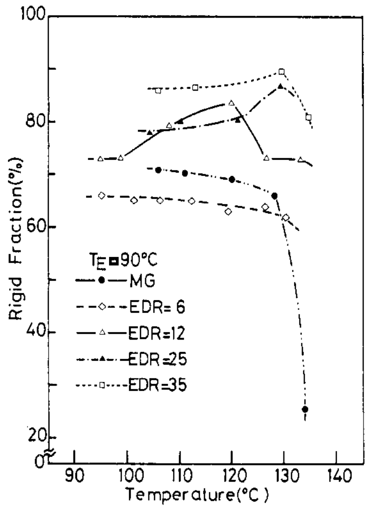

**Figure 6.** Temperature dependence of the $T_{2c}$ fraction, evaluated from the NMR signal intensity, for the extrudates extruded at 90 °C to different EDR.

The $T_{2c}$ fraction remains almost constant at lower temperatures for all the samples. At higher temperatures, where partial melting and reorganization may take place, each sample showed a characteristic behavior which varied depending on EDR. The $T_{2c}$ fraction of the MG sample decreases gradually and then sharply due to the onset of melting of the crystals. The EDR 6 extrudate showed a temperature dependence of $T_{2c}$ fraction similar to that of the MG sample. In contrast, a significant increase in $T_{2c}$ fraction was observed during NMR measurements for the extrudate with EDR 12. The initial value of $T_{2c}$ fraction remains about 72% below 100 °C and then begins to incrase until it reaches a maximum of 84% at 120 °C. Our experiments indicate that the difference between 72 and 84% crystallinity is significant. With further increase in temperature, the fraction decreases to a plateau value of 72%, which is the same as the initial value, and then decreases very rapidly due to melting. The effect of annealing at lower temperatures was studied by NMR. For this, the extrudate with EDR 12 was slowly heated to 113 °C, held there for 30 min, and cooled slowly to 85 °C. After this treatment, NMR data were obtained on the warming process. $T_{2a}$ increased significantly and the temperature where $T_{2i}$ component became observable decreased by 10 °C as a result of annealing. The $T_{2c}$ fraction at the low-temperature plateau value increased about 10%, in agreement with the previous result (Figure 6). The DSC thermogram for the extrudate with EDR 12 showed onset of melting at 127 °C with a peak temperature at 134.5 °C but no detectable change in heat capacity below 126 °C. This might be due to the difference in heating rate used for DSC (8 °C/min) and NMR measurements (~0.15 °C/min); the rate was too fast for the former but sufficiently slow for the latter to allow the sample to reorganize. However, it is known that DSC sometimes fails to detect such a structural reorganization which often occurs very rapidly during measurements with thermally metastable semicrystalline polymers composed of small or imperfect crystallites.[31-33] It is emphasized, however, that the crystallinity value measured by DSC is not substantially affected by such a reorganization because the increase in heat of fusion corresponding to the crystallinity increase during measurement is compensated by the heat evolved during the reorganization. It is noted that the $T_{2c}$ fraction observed in NMR corresponds to the mass fraction crystallinity at the measurement temperature.

The increase in $T_{2c}$ fraction during NMR measurements was most remarkable for EDR 12 with extrusion at 90 °C (Figure 6). At this stage of deformation, $T_{2a}$ approached, but was still greater than, the limiting shortest value. According to the Peterlin's model,[16,17] the initially spherulitic materials transform into fibrous morphology by drawing, and each fibril is composed of a number of microfibrils. The noncrystalline component exists either between two crystalline blocks as an amorphous layer within a microfibril or between fibrils or microfibrils.

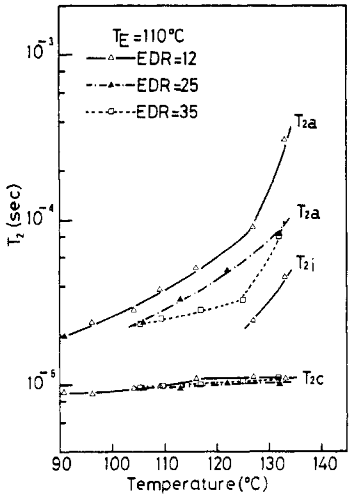

**Figure 7.** Temperature dependence of $T_2$ for the extrudates extruded at 110 °C with different EDR.

Further drawing proceeds mainly by interfibrillar shear slip, which increases the number and strain of the interfibrillar tie molecules. Our previous[28] and present studies (Table I) of these extrudates show that the crystalline orientation function ($f_c$) rapidly increases with EDR, reaching almost unity ($f_c > 0.98$) at an EDR of 10.[12] The increase in modulus with EDR is not, however, explained by this orientation alone. The EDR of 10 for extrusion at 90 and 110 °C corresponds to the critical EDR, after which the tensile modulus increases steadily with EDR.[12] This suggests that the latter mechanism becomes important at an EDR of 10 and is consistent with the NMR observation that $T_{2a}$ approaches the limiting shortest value at an EDR of 12. It is noted that $T_{2a}$ reaches a plateau for conditions somewhat different from those for the modulus. This may reflect the difference in the time scale for the two measurements. At this stage, the fairly extended long-chain interfibrillar tie molecules may not be strongly connected to the crystallites in a fibril as suggested by the fairly low modulus value.[12].

When EDR is increased further (EDR > 20), the structural reorganization during measurements is suppressed. The extrudate with the highest EDR, 35, has the highest thermal stability, and the fraction of $T_{2c}$ component remained almost invariant below 130 °C. According to small-angle X-ray diffraction, the long period does not significantly increase above EDR > 10.[28] However, more recent studies by wide-angle X-ray diffraction show that the crystallite size along the chain direction, estimated from the half-width of the (002) reflection, increases steadily at EDR > 10 and exceeded the long period at higher EDR.[34] Therefore, the improved thermal stability at high EDR may be attributed primarily to an extended-chain morphology. A detailed study of the morphological changes during extrusion will be reported in a separate paper.

**Effects of Extrusion Temperature.** It has been reported that the efficiency of extrusion drawing, as evaluated by the properties vs. EDR, is greatly influenced by the extrusion temperature.[3] Such variations may be reflected in the values of $T_{2a}$ and $T_{2i}$ and the fraction of the components. The relaxation times and the fraction of each component for the fibers extruded at 110 °C were measured and the results are shown in Figures 7 and 8. Comparison of the $T_2$ vs. temperature curves in Figures 3, 4, and 7 reveals that below 120 °C the fibers extruded at higher temperature have a slightly longer $T_{2a}$ at a given EDR. However, in the high-temperature region ($T > 120$ °C) the $T_{2a}$ values for both extrusion temperatures become almost identical by annealing at the measurement temperature. These results suggest that the noncrystalline component of the fibers extruded at higher temperature is in a slightly more relaxed state than those extruded at lower temperature. Although the fraction and the first appearance temperature of the $T_{2i}$ component are insensitive to the extrusion temperatures examined in this work, the $T_{2i}$ values are longer for the extrusion at higher temperature. These results suggest that the extrusion temperature has an important influence on the efficiency of draw for the noncrystalline regions of the extrudates. The extrusion at lower temperature produces more constraint on the molecular segments in the noncrystalline regions. Mead, Desper, and Porter[3] have extensively studied the effects of extrusion variables on the extrusion behavior and the resultant properties. They found that the efficiency of draw, as evaluated by the modulus vs. EDR, increases with decreasing extrusion temperature. The present result concerning amorphous-component behavior is in line with their finding.

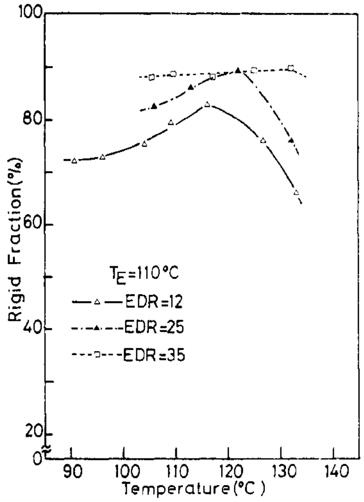

**Figure 8.** Temperature dependence of $T_{2c}$ fraction evaluated from the NMR signal intensity. Samples were extruded at 110 °C.

Ward[35] and others have carried out broad-line NMR studies on ultrahigh-modulus polyethylene and report that three components, broad, intermediate, and narrow, were observed in the spectra. They assigned these components to the crystalline regions, high molecular weight materials which interconnect the crystalline regions, and low molecular weight materials such as chain ends and cilia. At the beginning of this work, we also carried out broad-line NMR measurements on the samples used in the pulsed NMR study. The very narrow component reported by Ward et al. was not found in the spectra. This implies that the content of highly mobile materials is negligible in our samples. Indeed, the IR dichroism study[25] of the extrudate revealed that the molecular end groups exhibited fairly high orientation as evaluated by the orientation function of the end vinyl groups of HDPE. This difference might be due to the fact that we used polyethylene from different sources and that their samples were prepared by conventional drawing whereas ours were prepared by crystalline (solid) state extrusion under high pressure.

## Summary

Spin–spin relaxation times ($T_2$) in crystalline-state extruded high-density polyethylene, having a nominal EDR up to 35 and prepared at 90 and 110 °C, have been studied as a function of temperature by the solid echo NMR technique. Three relaxation times, $T_{2a}$, $T_{2i}$, and $T_{2c}$, assigned to the amorphous, intermediate, and rigid (crystalline) components, were observed for the melt-crystallized isotropic sample and extrudates with EDR ≤ 12. The highly drawn samples with EDR ≥ 25 exhibited only two $T_2$'s, i.e., $T_{2a}$, and $T_{2c}$. The structural change in noncrystalline regions that occurred during extrusion is sensitively detected by $T_{2a}$. The value of $T_{2a}$ decreased very rapidly with increasing EDR before EDR reached 12 and approached a plateau value at EDR > 12. This has the major implication that the constraint imposed on the noncrystalline component increases rapidly at EDR < 12 and reaches a limiting value at high EDR; further increase in EDR does not cause a significant change of the structure of noncrystalline regions in samples extrudedate ≤110 °C. The extrusion at lower temperatures produces more constraint on the molecular segments in the noncrystalline regions. The fraction of the $T_{2c}$ component was in good agreement with the mass fraction crystallinity estimated from the heat of fusion of the samples and increased with EDR. The sample having an intermediate EDR of 12 exhibited a significant increase in the $T_{2c}$ fraction as a result of annealing during NMR measurement. The thermal stability against annealing or melting also increased with EDR and the extrudate with the highest EDR, 35, showed no appreciable reorganization below 130 °C.

## References and Notes

(1) Desper, C. R.; Southern, J. H.; Ulrich, R. D.; Porter, R. S. *J. Appl. Phys.* **1970**, *41*, 4284.
(2) Capiati, N. J.; Porter, R. S. *J. Polym. Sci., Polym. Phys. Ed.* **1975**, *13*, 1177.
(3) Mead, W. T.; Desper, C. R.; Porter, R. S. *J. Polym. Sci., Polym. Phys. Ed.* **1979**, *17*, 859.
(4) Smook, J.; Torfs, J. C.; Hutten, P. F.; Penning, A. J. *Polym. Bull.* **1980**, *2*, 293.
(5) Capaccio, G.; Ward, I. M. *Nature (London), Phys. Sci.* **1973**, *243*, 143.
(6) Capaccio, G.; Ward, I. M. *Polymer* **1974**, *15*, 233.
(7) Southern, J. H.; Porter, R. S. *J. Appl. Polym. Sci.* **1970**, *14*, 2305.
(8) Porter, R. S.; Southern, J. H.; Weeks, N. *Polym. Eng. Sci.* **1975**, *15*, 213.
(9) Mead, W. T.; Porter, R. S. *J. Appl. Phys.* **1976**, *47*, 4278.
(10) Clements, J.; Capaccio, G.; Ward, I. M. *J. Polym. Sci., Polym. Phys. Ed.* **1979**, *17*, 693.
(11) Porter, R. S.; Weeks, N. E.; Capiati, N. J.; Krzewki, R. J. *J. Thermal Anal.* **1975**, *8*, 547.
(12) Kanamoto, T.; Sherman, E. S.; Porter, R. S. *Polym. J.* **1979**, *11*, 497.
(13) Arridge, R. G. C.; Barham, P. J.; Keller, A. *J. Polym. Sci., Polym. Phys. Ed.* **1977**, *15*, 389.
(14) Imada, K.; Yamamoto, T.; Ueno, K.; Matsukuma, D.; Takayanagi, M. *J. Soc. Mater. Sci. Jpn.* **1970**, *19*, 302.
(15) Imada, K.; Yamamoto, T.; Shigematsu, K.; Takayanagi, M. *J. Mater. Sci.* **1971**, *6*, 537.
(16) Peterlin, A. *J. Mater. Sci.* **1971**, *6*, 490.
(17) Peterlin, A. *Polym. Eng. Sci.* **1979**, *19*, 118.
(18) Fujimoto, K.; Nishi, T.; Kado, R. *Polym. J.* **1973**, *3*, 448.
(19) McBrierty, V. J. *Polymer* **1974**, *15*, 503.
(20) Ito, M.; Serizawa, H.; Tanaka, K. *Polym. J.* **1978**, *10*, 215.
(21) Powles, J. G.; Strange, J. H. *Proc. Phys. Soc. London* **1963**, *82*, 6.
(22) Griswold, P. D.; Zachariades, A. E.; Porter, R. S. Presented at the Stress-Induced Crystallization Symposium, Midland Macromolecular Institute, Midland, MI, Aug 1977.
(23) Wunderlich, B.; Cormier, C. M. *J. Polym. Sci., Part A-2* **1967**, *5*, 987.
(24) Nakayama, K.; Kanetsuna, H. *J. Mater. Sci.* **1975**, *10*, 1105.
(25) Miller, P. J.; Jackson, J. F.; Porter, R. S. *J. Polym. Sci., Polym. Phys. Ed.* **1973**, *11*, 2001.
(26) Wu, W.; Simpson, P. G.; Black, W. B. *J. Polym. Sci., Polym. Phys. Ed.* **1980**, *18*, 751.
(27) Peterlin, A.; Williams, J. L.; Stannett, V. *J. Polym. Sci., Part A-2* **1967**, *5*, 957.
(28) Kanamoto, T.; Kadowaki, I.; Tanaka, K.; Porter, R. S. Presented at the Annual Meeting, Polymer Science in Japan, Kyoto, May 1980.
(29) Sumita, M.; Miyasaka, K.; Ishikawa, K. *J. Polym. Sci., Polym. Phys. Ed.* **1977**, *15*, 837.
(30) Dhawan, K.; Chanbey, D. R.; Yadav, Y. S. *Polym. J.* **1980**, *12*, 411.
(31) Bair, H. E.; Salovey, R.; Huseby, T. W. *Polymer* **1967**, *8*, 9.
(32) Harrison, I. R. *J. Polym. Sci., Polym. Phys. Ed.* **1973**, *11*, 991.
(33) Ito, M.; Kanamoto, T.; Tanaka, K. *Bull. Chem. Soc. Jpn.* **1977**, *50*, 967.
(34) Kanamoto, T., to be submitted for publication.
(35) Smith, J. B.; Manuel, A. J.; Ward, I. M. *Polymer* **1975**, *16*, 57.